RESEARCH ARTICLE

Hybrid Dynamic Phasor Modeling Approaches for Accurate Closed-Loop Simulation of Power Converters

SRIRAM KARTHIK GURUMURTHY[1]**, (Member, IEEE), MARKUS MIRZ**[1,2]**,
BERNARD S. AMEVOR**[1]**, FERDINANDA PONCI**[1]**, (Senior Member, IEEE),
AND ANTONELLO MONTI**[1]**, (Senior Member, IEEE)**

[1]E.ON Energy Research Center, Institute for Automation of Complex Power Systems, RWTH Aachen University, 52062 Aachen, Germany
[2]Digital Energy, Fraunhofer FIT, 53757 Aachen, Germany

Corresponding author: Sriram Karthik Gurumurthy (sgurumurthy@eonerc.rwth-aachen.de)

ABSTRACT Modelling the fast dynamics of power converters is of growing concern in power grids and Microgrids. Dynamic phasor (DP) concept has been widely applied to switched power converter for modelling fast transients efficiently due to the inherent frequency shift property of DPs. The dynamics introduced by the DC/AC power converters depend on the controllers, which are implemented either in the stationary frame or on the synchronous reference frame (SRF). Hybrid closed-loop modelling methods that consider DP-based power converter plant model are not established and the applicability and accuracy of such hybrid approaches are not fully understood. This paper attempts to address this gap by proposing two hybrid closed-loop modelling approaches: Hybrid DP-DQ and Hybrid DP-EMT and discusses the applicability and accuracy for various controller types. Furthermore, this paper presents a DP switched model of single and three phase two level power converter and discusses the selection of harmonics to reduce model complexity. The proposed hybrid approaches were validated against detailed switched power converter models and for a wide range of scenarios, the Hybrid DP-EMT method is found to be superior compared other methods. Finally, application dependent recommendations are made for the selection of suitable hybrid closed-loop model for the accurate simulation of single phase and three phase power converters.

INDEX TERMS Control systems, digital twin, dynamic phasor, energy conversion, environment control system, modelling, more electric aircraft, power electronics, power converter, simulation, synchronous reference frame.

I. INTRODUCTION

There has been a subsequent push in the aviation industry to move towards more electric aircraft (MEA). The primary motivations are similar to that of electric vehicles i.e. reduce CO2 emissions and to minimize fuel consumption [1]. With MEAs, most of the subsystems that use non-electric energy conversion are replaced with electrical energy conversion systems. An example of such an MEA concept can be found

in the Environment Control System (ECS) of Boeing 787. The ECS system is responsible for maintaining cabin temperature and pressure and conventionally it was achieved by tapping bleed air off one of the compressor stages of the main engines. However, in Boeing 787, a dedicated set of compressors which utilize electrical power maintain cabin temperature and pressure thereby eliminating need for pneumatic systems [1]. Among popular commercial MEAs such as Boeing 787 and Airbus A380, the aircraft power system (APS) uses a constant voltage variable frequency bus unlike conventional APS which used a conventional constant voltage constant

The associate editor coordinating the review of this manuscript and approving it for publication was Xiaodong Liang.

frequency bus [1], [2]. The variable frequency bus concept has created tremendous requirements for power converters in terms of control, stability, power quality, power filter topologies, overall size and weight [1], [3]. Power quality and stability are extremely critical and specifically the study of harmonics and their coupling within the APS is of utmost importance [3].

Simulation of power electronics dominated APS in a detailed manner may be time consuming with conventional EMT switched models. Furthermore, the design of such complex APS can be benefited by simulation tools which can simulate the system with high accuracy and at a fast rate. Within the scope of Clean Sky 2 Joint Undertaking (JU) funded project TWINECS, one of the important goals is to create closed loop detailed simulations of power converters. This paper considers grid-connected single phase and three phase power converters operating in inverter mode. This paper aims to develop hybrid closed-loop Dynamic Phasor (DP) models of power converters to achieve an accurate representation in transient behaviour.

In conventional time domain (TD) or Electromagnetic Transient (EMT), the switching events within a power converter are captured in numerical simulation by adopting a very small time step. The accuracy in EMT simulations is high, however the computation complexity is proportionally high. On the other hand, steady state phasor based simulation is very fast but inaccurate for capturing transient behavior. DP based simulation enables increased simulation step sizes and a decreased overall execution time when compared to conventional EMT solvers.

DPs are the time-varying Fourier complex coefficients of a signal [4], [5], [6], [7]. The dynamic phasor concept was initially referred to as Generalized State Space Averaging (GSSA) which was first introduced in [4] where it was applied for a variety of switched circuits. The DP modelling method applied to DC/DC converters [5], [6], [7] and DC/AC converters such as three phase inverters [8], [9], [10], [11], [12], [13], MMCs [14] and other power electronics such as Auto Transformer Rectifier Unit (ATRU) [12] do not propose strategies to reduce model complexity and do not provide recommendations of a selection criteria for harmonics. Furthermore, the methods used to represent the controller and the domain used to simulate the controller is not described. Recently, DP based models were applied for AC Microgrids for simulation and study of eigen values unbalanced conditions [15], [16]. However, the switched behavior of the converter was neglected and only an averaged duty cycle was considered. Such models fail to capture the harmonic instability phenomenon or parallel resonance phenomenon which occurs mainly due to inter-harmonics arising from the interaction between the converter and grid [17], [18].

The basic idea in our work is to express the switched time-domain voltage waveform of a power converter in terms of Fourier series and consider only the significant harmonics. Each frequency component in the switched voltage waveform can be expressed as a DP variable. Each energy storage element can be defined with one complex-valued state equation or two real-valued state equations when considering the real and imaginary part separately. By considering only those frequency components which are greater than a pre-defined threshold, the number of harmonics and its corresponding equations can be significantly reduced. Transformation of time-domain switched voltage waveforms of DC/AC power converters to Fourier coefficients results in mathematical expressions containing Bessel function of first kind. The number of terms within the Bessel function summation series to accurately model the phasor needs to be pre-calculated. Due to the shifted frequency nature of DPs, the time steps can be significantly increased leading to faster simulations [19]. In this work, we have developed a detailed dynamic phasor based switched model of a single phase and a three phase two-level power converter with multiple frequency components. Selection criteria for harmonics are presented along with the selection of number of terms in the Bessel function infinite sum. This paper also presents hybrid modelling approaches for controllers that are suitable for closed-loop simulation of DP based power converter model. The two hybrid modelling approaches proposed in this work are: Hybrid DP-DQ and Hybrid DP-EMT method. Furthermore, we evaluate the applicability of these hybrid modelling approaches for different controller types and for different converter type. This paper presents the applicability and accuracy of the hybrid modelling approaches. The simulation results obtained by the proposed Hybrid DP approaches are compared to the simulation results obtained by EMT simulation through the normalized root mean square error (NRMSE) evaluation.

Within the context of simulating large networks, hybrid approaches have been proposed wherein the system is partitioned into multiple subsystems [20], [21], [22]. Typically, the subsystem containing the converter is modelled in the DP domain and the other subsystems are modelled in the EMT domain. Recently, such a hybrid model was proposed for simulating HVDC networks [20]. Other hybrid simulation methods that use static or dynamic phasors and EMT can be found in [21] and [22]. A major difference between this literature and our work is that we focus on the development of hybrid closed-loop modelling approaches within the different subsystems of the power converter. The hardware part of the power converter is modelled in the DP domain whereas the controller part is modelled either in DP domain (Fully DP method) or in time domain (Hybrid DP-DQ, Hybrid DP-EMT methods). In this paper, controllers operating on different frames of references such as synchronous reference frame (SRF) and the stationary frame are considered and we evaluate the proposed hybrid approaches in terms of its simulation accuracy in transients.

The contributions of this paper are:
- Development of the dynamic phasor switched model of a single phase and three phase two level converter
- Strategies to reduce the complexity in dynamic phasor switched power converter models are proposed such as: a) Selection of dominant switching frequency

component, b) Selection of number of bessel function terms
- Hybrid modelling methods: Hybrid DP-DQ and Hybrid DP-EMT methods for closed loop simulation of power converters within the dynamic phasor framework are proposed. The accuracy and applicability of hybrid approaches are presented for different controller types

The rest of the paper is organised as follows: Section II summarizes the theory of dynamic phasors. Description of DP based switched power single and three phase inverter models are presented in Section III. Section IV represents the various hybrid approaches for the closed loop simulation of the DP-based switched power converter models. Section V discusses the application and complexities of the various hybrid modelling approaches for different controller types. The simulation results and validation of models are presented in Section VI and finally the conclusion and remarks on the future work are presented in Section VII.

II. THEORY OF DYNAMIC PHASORS

Dynamic phasors can be understood as the complex envelopes of passband signals. The complex envelope or complex baseband signal is calculated from the analytic representation of a signal shifted in frequency.

$$\langle \psi \rangle (t) = \psi_a(t)e^{-j\omega_s t} \tag{1}$$

The analytic representation of a signal is composed of the original signal and its Hilbert transform as shown in (2) [23].

$$\psi_a(t) = \psi(t) + j\mathcal{H}(\psi(t)) \tag{2}$$

The Hilbert transformation applied to a real-valued signal is defined by (3). Under the Hilbert transformation, a real-valued signal undergoes a phase shift (lag) by 90 degree.

$$\mathcal{H}(\psi(t)) = \frac{1}{\pi} \int_{-\infty}^{+\infty} \frac{\psi(\tau)}{t - \tau} d\tau \tag{3}$$

To retrieve the original signal, the imaginary part is omitted from the analytic representation. If the signal is represented by a dynamic phasor, it is necessary to reverse the frequency shift and if the phasor signal has been sampled, interpolation might be required. If a signal is decomposed into its harmonic constituents, it is retrieved by omitting the imaginary part of the of sum the dynamic phasors shifted in reverse,

$$\psi(t) = \Re \left\{ \sum_{k=-\infty}^{\infty} \langle \psi \rangle_k(t) e^{jk\omega_s t} \right\} \tag{4}$$

where k is the harmonic index. The dynamic phasors $\langle \psi \rangle_k(t)$ can also be approximated using the Fourier transform. The time dependency of the phasor can be modelled by using the time-dependent formula of the Fourier series integral. Assuming a sliding observation window with period T moving along the time axis, the time dependent Fourier coefficients are expressed by the transform (5), where ω_s is the fundamental frequency.

$$\langle \psi \rangle_k(t) = \frac{1}{T} \int_{t-T}^{t} \psi(\tau) \cdot e^{-jk\omega_s \tau} d\tau \tag{5}$$

Power-electronic converters are modeled as first order differential equations in order to realize the state space representation including the output filter. The first order differentiation operator for dynamic phasors is given by (6).

$$\frac{d}{dt}\langle \psi \rangle_k(t) = \left\langle \frac{d}{dt}\psi \right\rangle_k(t) - j\omega_s k \langle \psi \rangle_k(t) \tag{6}$$

The product of two dynamic phasors, x and y is calculated through the discrete convolution principle given by (7).

$$\langle xy \rangle_k = \sum_{i=-\infty}^{\infty} \langle x \rangle_{k-i} \langle y \rangle_i \tag{7}$$

Without loss of generality, the resulting equations modelled using the dynamic phasor concept of a generic power electronic converter can be non-linear of the form (8).

$$\frac{d\langle \psi \rangle_k}{dt} = f(\langle \psi \rangle_k, \langle u \rangle_k) \tag{8}$$

The control signal $\langle u \rangle_k$ produced by the controller can be expressed either in the dynamic phasor domain or in the original time domain. For closed loop power electronic converter simulation, two methods are discussed: Fully DP and Hybrid DP. These methods are discussed in detail in Section IV.
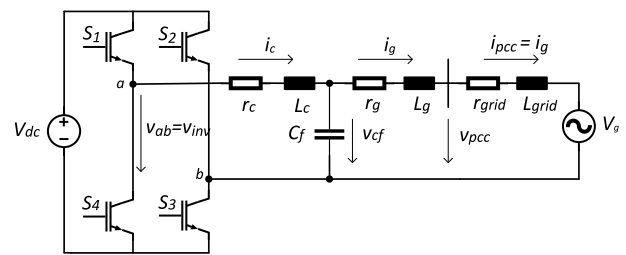

FIGURE 1. Diagram of single phase inverter.

III. DP BASED SWITCHED POWER CONVERTER MODEL
A. SINGLE PHASE INVERTER
This paper presents a switching function based dynamic phasor model of a single phase inverter. Fig. 1 shows the topology of a single phase inverter with LCL filter. The converter side inductor and grid side inductor are L_c and L_g respectively, their internal resistances are r_c and r_g respectively and the filter capacitance is C_f. A resistive-inductive grid impedance consisting of elements r_{grid} and L_{grid} is assumed to exist between the point-of-common-coupling (PCC) and the grid. In order to capture the switching harmonics of the inverter and its sideband harmonics, the inverter output voltage v_{inv} needs to be modelled with an appropriate switching function, which depends on the type of modulation used. Unipolar modulation is considered for the generation of sine triangle modulated pulses for switching the power-electronic switches. Ideal switch model assumption is considered and the internal charge dynamics such as reverse recovery effects and tail currents are neglected. Additionally, snubber circuits are also not considered. Under unipolar modulation, the switching takes place between voltage levels $+V_{dc}$ and 0 during the
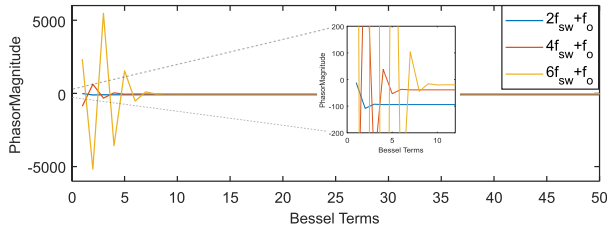
FIGURE 2. Required number of terms k in the Bessel Function to accurately model the switching function.

FIGURE 3. Required bessel function terms for various switching and grid harmonics.

positive half-cycle and between 0 and $-V_{dc}$ during negative half-cycles.

The indices m and n refer to harmonics of the switching frequency $\omega_s = 2\pi f_s$ and the harmonics of the fundamental frequency $w_o = 2\pi f_o$ respectively. Considering a regularly sampled double edged unipolar modulation, the side band harmonics ω_{mn} of the inverter voltage v_{inv} exists at integer multiples of the switching frequency and odd multiples of fundamental frequency. The sideband harmonics can be generalised as
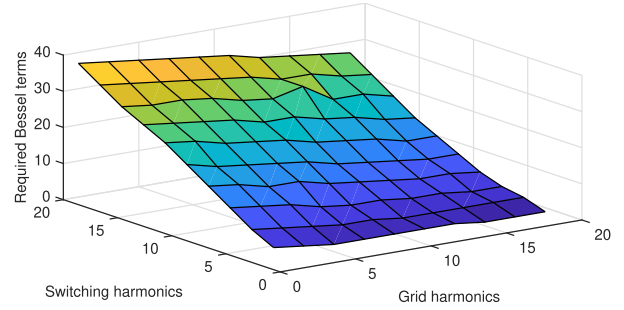
$$\omega_k = m\omega_s + (2n-1)\omega_o, \quad (9)$$

where $m \in \mathbb{N}$ and $n \in \mathbb{Z}$. The switching function of the single phase inverter with unipolar modulation is obtained by applying double Fourier series expansion of the voltage waveform between the midpoints of the two phase legs $v_{inv}(t)$ [8] and assuming regular sampling double edge carrier, it is given by (10),

$$
\begin{aligned}
v_{inv}(t) =\ & \frac{4V_{dc}}{\pi} \sum_{n=1,3,..} \frac{J_n\left(n\frac{\omega_o}{\omega_{sw}}\frac{\pi}{2}M_r\right)}{\left[n\frac{\omega_o}{\omega_{sw}}\right]} \\
& \times \sin\left(n\left[1+\frac{\omega_o}{\omega_{sw}}\right]\frac{\pi}{2}\right) \cos(n\omega_o t + n\varphi) \\
& + \frac{4V_{dc}}{\pi} \sum_{m=1,2,..} \sum_{n=\pm1,\pm3,..} \frac{J_n\left(\left[m+n\frac{\omega_o}{\omega_{sw}}\right]\frac{\pi}{2}M_r\right)}{\left[m+n\frac{\omega_o}{\omega_{sw}}\right]} \\
& \times \sin\left(\left[m+n\frac{\omega_o}{\omega_{sw}}+n\right]\frac{\pi}{2}\right) \cos(m\omega_{sw} t + n\omega_o t)
\end{aligned}
$$
$$(10)$$

where M_r is the modulation ratio, φ is the phase of the control reference signal and J_n is the Bessel function of the first kind expressed as,

$$J_n(x) = \sum_{p=0}^{\infty} \frac{(-1)^p}{p!\Gamma(p+n+1)} \left(\frac{x}{2}\right)^{2p+n}. \quad (11)$$

Here, p represents the number of terms required in the Bessel function and Γ represents the Gamma function which is defined as $\Gamma(p) = (p-1)!$. The Bessel function comprises an infinite number of terms. However, the effective number of terms that is sufficient to model the switching function be determined by calculating the phasor magnitude of the highest sideband frequency of interest for various Bessel

function terms. As the number of terms of Bessel function is increased, the convergence in the phasor magnitude can be observed. Fig. 2 plots the phasor magnitudes and number of terms used in the Bessel function for different phasors. Fig. 2 shows that as p increases, the approximation of the Bessel function improves. Furthermore, higher frequencies require more terms for convergence and for the example considered, the frequency $6f_{sw} + f_o$ requires around 12 terms. The number of terms required in the bessel function computation is determined for every harmonic such that the absolute error in the phasor magnitude and phase angle are less than 1 percent of the reference value. The reference value is computed by considering arbitrarily large p such that the Bessel function has converged. Fig. 3 shows the number of bessel function terms required for various grid harmonics and switching harmonics. From Fig. 3, it can be inferred that the dependency of the bessel function on the switching harmonic m is significant than the grid harmonic n. In this paper, we have considered $m = 6$ and $n = 5$ and thus for improved accuracy, $p = 20$ is considered for the reminder of the paper.

Applying (5) with $\omega_k = m\omega_s + n\omega_0$ and the corresponding time period as $T_{mn} = \frac{2\pi}{\omega_k}$ to (10) results in the DP phasor switched model of the single phase inverter given by (12), as shown at the bottom of the next page. The switched voltage waveform v_{inv} obtained by post processing the DPs corresponding to $m = 6$ and $n = 5$ is shown in Fig. 4 where the simulated inverter voltage from Simulink is plotted. The frequency spectrum of both DP and time domain simulation accurately match.

The LCL filter model at the output of the inverter can be modelled in DP domain. When integrating the single phase inverter model with software tools such as DPSim, the LCL filter model is typically considered part of the power network which is modelled via Modified Nodal Analysis (MNA). However for sake of clarity, the DP phasor model of the output filter is given below:

$$\frac{d\langle i_c \rangle_k}{dt} = \frac{\langle v_{inv} \rangle_k}{L_c} - \frac{\langle v_{cf} \rangle_k}{L_c} - \frac{\langle i_c \rangle_k r_c}{L_c} - j\omega_k \langle i_c \rangle_k \quad (13)$$

$$\frac{d\langle v_{cf} \rangle_k}{dt} = \frac{\langle i_c \rangle_k}{C_f} - \frac{\langle i_g \rangle_k}{C_f} - j\omega_k \langle v_{cf} \rangle_k \quad (14)$$
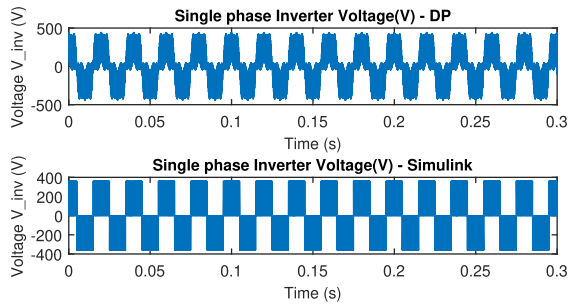
FIGURE 4. Single phase converter output voltage comparison.
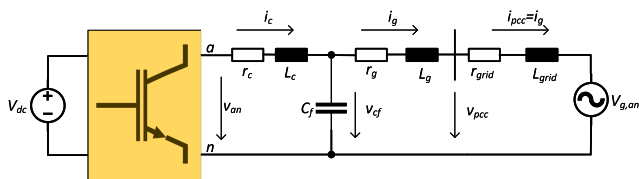

FIGURE 5. Diagram of three phase inverter.

$$\frac{d\langle i_g \rangle_k}{dt} = \frac{\langle v_{cf} \rangle_k}{L_g + L_{grid}} - \frac{\langle v_g \rangle_k}{L_g + L_{grid}}$$
$$- \frac{\langle i_g \rangle_k (r_g + r_{grid})}{L_g + L_{grid}} - j\omega_k \langle i_g \rangle_k \qquad (15)$$

In the above equations, w_k refers to the set of all considered switching and side-band harmonics $m\omega_s \pm n\omega_o$. The PCC voltage phasor can be calculated using (16).

$$\langle v_{pcc} \rangle_k = \langle v_g \rangle_k + \langle i_g \rangle_k (r_{grid} + j\omega_k L_{grid}) \qquad (16)$$

B. THREE PHASE INVERTER
Consider a three phase converter with B6C topology as shown in Fig. A similar output LCL filter structure is considered at every phase. Consider a sine pulse width modulation (SPWM) strategy for generating the gate pulses with a triangular carrier wave. Furthermore, for the sampling of PWM, consider the natural sampling based double edge carrier. From the above mentioned assumptions on the PWM, the time domain waveform of the phase - neutral voltage can be calculated [8], [9]. Phase-neutral voltage of Phase A $v_{an}(t)$ can be calculated suing double Fourier series as shown in (17). Here, m represents the harmonics of switching frequency ω_{sw} and n represents the harmonics of fundamental frequency ω_o. Thus, the frequency points $m\omega_{sw} + n\omega_o$ represent the side band harmonics. From (17), it can be inferred the harmonics in the phase-neutral voltage vanishes if n is a

multiple of 3 or if $m + n$ is even.

$$v_{an}(t) = \frac{M_r V_{dc}}{2} cos(\omega_o t + \varphi) + \frac{4V_{dc}}{3\pi} \sum_{m=1}^{\infty} \sum_{n=-\infty}^{\infty}$$
$$\times \frac{J_n\left(mM_r \frac{\pi}{2}\right)}{m} \sin\left(\left[m+n\right]\frac{\pi}{2}\right)\left(1 - \cos\left(\frac{2\pi n}{3}\right)\right)$$
$$\times cos\left(\left[m\omega_{sw} + n\omega_o\right]t + n\varphi\right) \qquad (17)$$

By applying the Fourier integral (5) to (17), the dynamic phasor of phase A voltage $\langle v_{an} \rangle_k(t)$ is derived as shown in (18), at the bottom of the next page.

Phase to neutral voltages of other phases can be obtained by phase shifting the A phase phasor under balanced assumption as shown below:

$$\langle v_{bn} \rangle_k = \langle v_{an} \rangle_k e^{-j\frac{2\pi}{3}}$$
$$\langle v_{cn} \rangle_k = \langle v_{an} \rangle_k e^{j\frac{2\pi}{3}}$$

Similar to the single phase case, the three phase output voltage post processed from DPs corresponding to $m = 6$ and $n = 5$ is plotted in Fig. 6. The spectrum obtained from Simulink accurately matches magnitudes of the DPs.

IV. CLOSED LOOP DYNAMIC PHASOR MODELING APPROACHES
The controllers of power converters are typically implemented either in the stationary frame or in the synchronous reference frame (SRF). In this paper, we are considering DP models of power converters (plant model). The controllers can be modelled either in the DP domain or in time-domain. The modelling domain adopted for different controllers types to achieve accurate transient response as compared with a conventional EMT time domain simulation needs to be established. This section presents three approaches for closed loop modelling and simulation of dynamic phasor based power converter models: Fully DP, Hybrid DP-DQ and Hybrid DP-EMT.

A. FULLY DP
In the Fully DP approach, both the controller and the plant are in the DP domain as shown in Fig. 7. The control input $\langle e \rangle_k$ can be expressed as a phasor at each frequency k [24]. The control input can be multiplied with the complex valued gain of the controller at the corresponding frequency to compute the controller output phasors.

$$\langle u \rangle_k = \langle C \rangle_k \langle e \rangle_k \qquad (19)$$

$$\langle v_{inv} \rangle_k = \begin{cases} \dfrac{2V_{dc} J_n\left(\pi n \frac{\omega_o}{\omega_{sw}} \frac{\pi}{2} M_r\right)}{\pi n \frac{\omega_o}{\omega_{sw}}} \sin\left(n[1 + \frac{\omega_o}{\omega_{sw}}]\frac{\pi}{2}\right) e^{(jn\varphi)} & \text{for } n = 3, 5, \cdots ; m = 0 \\[20pt] \dfrac{2V_{dc} J_n\left([m + n\frac{\omega_o}{\omega_{sw}}]\frac{\pi}{2} M_r\right)}{\pi[m + n\frac{\omega_o}{\omega_{sw}}]} \sin\left([m + n\frac{\omega_o}{\omega_{sw}} + n]\frac{\pi}{2}\right) & \text{for } m \in \{I^+\}; n \in \{I - 0\} \end{cases} \qquad (12)$$
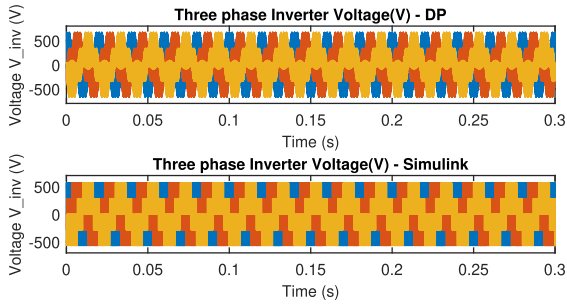
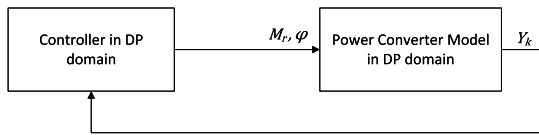**FIGURE 6.** Three phase converter phase-neutral output voltage comparison.

FIGURE 7. Fully DP.

When the controllers are implemented in the DQ-domain, the main contributor to control signal is the phasor corresponding to fundamental harmonic. The higher order harmonics as observed from the DQ domain are perceived either 50 Hz above or below their respective frequencies depending on whether the harmonic corresponds to a positive or negative sequence respectively. For example, a 500 Hz phasor, following the positive sequence is observed as a 450 Hz phasor in DQ domain and at 550 Hz when following the negative sequence and Table 1 summarises this concept. Hence the DQ control signals are calculated as

$$\langle u \rangle(t) = \langle u \rangle_o(t) \ + \sum_k \underbrace{\langle u \rangle_k(t) \, e^{j(\omega_k - \omega_o)t}}_{u'_k(t)} . \quad (20)$$

TABLE 1. Original sequence to DQ domain.

Phasor Frequency	Positive Sequence	Negative Sequence
ω_k	$\omega_k - \omega_o$	$\omega_k + \omega_o$

An exemplary path traced out by the control phasor in time in the DQ space is depicted in Fig. 8. At a given steady state, the control phasor at the fundamental is constant, however, due to the higher harmonics, the resultant phasor is time-varying as shown in Fig. 8. When the impact of higher harmonics on the control signals are neglected, typically through a low pass filter assumption then the control signal equals $\langle u \rangle_o$. Calculation of the modulation index M_r and the
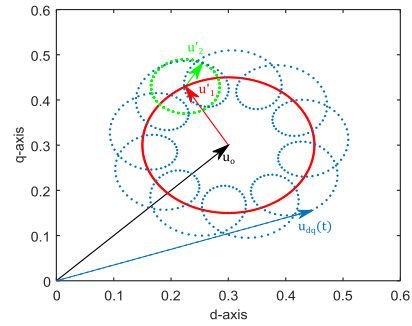

FIGURE 8. Control signal modelling in DP domain.

phase shift ϕ is obtained from the control signal.

$$M_r = \frac{\sqrt{\langle u \rangle_{re}^2 + \langle u \rangle_{im}^2}}{V_{sc}} \quad (21)$$

$$\varphi = \arctan\left(\frac{\langle u \rangle_{re}}{\langle u \rangle_{im}}\right) \quad (22)$$

The scaling voltage in the denominator $V_{sc} = V_{dc}$ for single phase converters and $V_{sc} = \frac{V_{dc}}{2}$ for three phase converters.

Linear controllers can be modelled in a straightforward manner and non-linear controllers require the usage of discrete convolution principle given in (7) to express product and or higher powers of periodic time domain variables such as state variables and switching functions. Thus, such a method possesses complexity towards modelling non-linear controllers. Due to the disadvantages of increased complexity in modelling non-linearities, hybrid approaches are necessary.
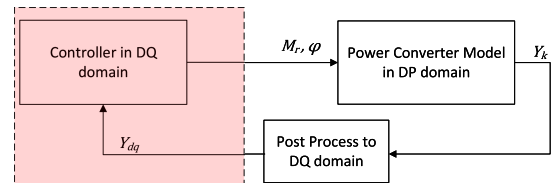

FIGURE 9. DP-DQ.

B. HYBRID DP-DQ

Fig. 9 shows the Hybrid DP-DQ implementation where the controller is implemented in DQ domain and the plant model is the DP domain. A typical usecase for this application is when the controller is implemented as a vector control such as the DQ domain controller. Since the plant outputs are phasors, post-processing is required to convert the DPs to DQ domain. This post processing can be achieved in two steps. The first

$$\langle v_{an} \rangle_k = \begin{cases} \dfrac{M_r V_{dc}}{4} e^{j\varphi} & \text{for } m = 0 \text{ and } n = 1 \\[2ex] \dfrac{2 V_{dc} J_n(m M_r \pi/2)}{3\pi m} \sin\left([m+n]\dfrac{\pi}{2}\right)\left(1 - \cos\left(\dfrac{2\pi n}{3}\right)\right) e^{jn\varphi} & \text{for } m = 1, 2, 3, \cdots \text{ and } n = \cdots, -1, 0, 1, \cdots \end{cases} \quad (18)$$

step involves converting the DPs to positive sequence space-phasors by the transformation in (23).

$$\langle i_g \rangle_k = \frac{2}{3} \begin{bmatrix} 1 & \alpha & \alpha^2 \end{bmatrix} \begin{bmatrix} \langle i_a \rangle_k \\ \langle i_b \rangle_k \\ \langle i_c \rangle_k \end{bmatrix} \quad (23)$$

The second step is the calculation of DQ domain signals from the space-phasors as given in (24) which is similar to (20). In the case of single phase converters, conversion to space-phasors is not necessary and (24) can be directly implemented.

$$i_{g,dq}(t) = \langle i_g \rangle_0 + \sum_k \langle i_g \rangle_k e^{j(\omega_k - \omega_o)t}. \quad (24)$$

The output of controller is in DQ domain which can be used to calculate and update M_r and φ. The Hybrid DP-DQ method does not account for the delays or additional signal processing that may occur outside the DQ domain such as filtering the measured stationary frame signals, delays in obtaining stationary frame signals and delays in conversion of stationary rame signals to DQ domain.
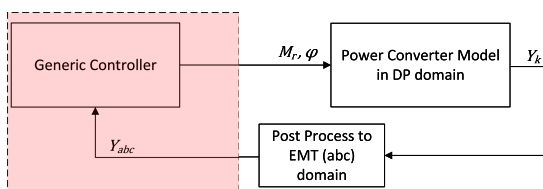
FIGURE 10. DP-EMT.

C. HYBRID DP-EMT

Mitigation of the disadvantages in Hybrid DP-DQ approach can be achieved by implementing the controller in the EMT domain. Within the Hybrid DP-EMT approach as shown in Fig. 10, the controller is implemented in EMT domain and the plant is implemented in DP domain. Post processing of the plant output phasors to EMT domain is realized via (4). In Hybrid DP-EMT method, the control implementation mimics reality as how it is implemented in an embedded platform.

To illustrate the steps in the proposed hybrid methods, a flowchart is shown in Fig. 11. Step 1 is the initialisation phase where the states of the system are initialized and the phasors of the power converter are initialized by assuming a fixed modulation ratio and angle at time $t = 0$. Steps 2 to 4 are repeated until the end of simulation. In step 2, the system of equations in DP domain is solved and the DP state variable output can be obtained. In Step 3, the DPs are interpolated and post-processed to time domain. Interpolation of DPs are required when the time domain signal is required with a much smaller time step compared to the time step used to solve the DP state equations. Using the time domain signal, the control inputs are calculated in the time domain following which the phasor voltages of the converter are calculated in Step 4.
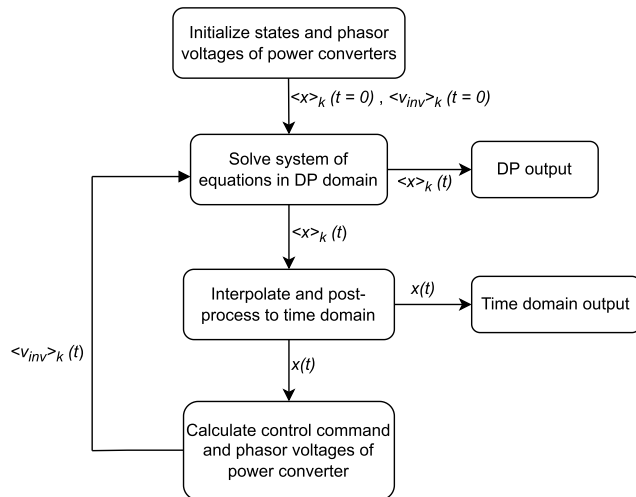
FIGURE 11. Simulation flowchart for Hybrid DP-DQ and Hybrid DP-EMT approaches.

V. APPLICATION OF HYBRID MODELING APPROACHES FOR POWER CONVERTERS

This section discusses the applicability of hybrid modelling approaches for various controller types.

A. CONTROLLERS CONSIDERED FOR THE ANALYSIS

We have considered three controllers in this paper: SRF-PI controller, SRF-SMC controller and a stationary PR controller. We consider discritzed implementation of the aforementioned controllers. Trapezoidal method is chosen to discritize the controller. As shown in Fig. 13. It is assumed that currents and voltages are sampled at instance λ and the control calculation is performed within the sampling interval T_s following which the control signal is updated at $\lambda + 1$.
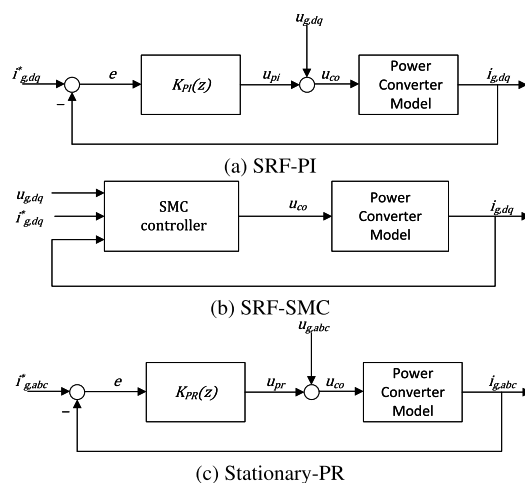
FIGURE 12. Controller.

The SRF-PI controller is implemented in the DQ-domain as shown in Fig. 12a. The current reference is tracked through

two PI controllers and a PCC voltage feedforward.

$$u_{pi}(\lambda) = u_{pi}(\lambda - 1) + \left(K_p + \frac{K_i T_s}{2} \right) e(\lambda) \\ + \left(-K_p + \frac{K_i T_s}{2} \right) e(\lambda - 1) \quad (25)$$

The control input is calculated along with the feed-forward term $u_{co} = u_{pi} + u_{g,dq}$. The simplified SRF-SMC current controller considered in this paper takes the form in (26). The control law was designed by simplifying the LCL filter to an L filter where R_T and L_T are the total series resistance and inductance of the LCL filter. The smoothed sliding surface is represented by the inverse tangent of the error function and K_{smc} represents the tunable control parameter.

$$u_{co} = u_{g,dq} + R_T i_{g,dq} - j\omega_o L_T i_{g,dq} + K_{smc} \tan^{-1}(e) \quad (26)$$

Implementation of stationary PR controller in the EMT domain is straightforward by using a state space approach. Implementing a stationary PR controller in the DQ domain has been discussed in previous works [25], [26]. Considering only the fundamental component, the stationary PR controller can be equivalently modelled equivalent as a synchronous frame DQ controller [25]. However, considering wider frequency response and considering both positive, negative sequence components, the equivalent synchronous frame control can be be calculated as proposed in [26].
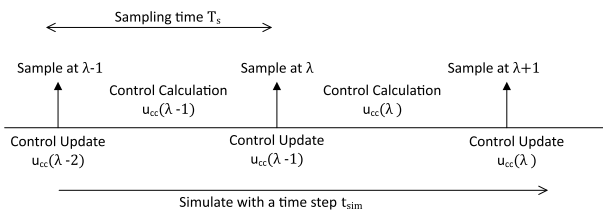
FIGURE 13. Controller sampling and update.

B. APPLICATION TO SINGLE PHASE POWER CONVERTERS

Consider the single phase inverter to controlled using a synchronous reference frame (SRF) controller with grid voltage feed-forward. Conventionally, SRF is not defined for single phase systems. However, thanks to digital implementations, the split-phase technique can be used as shown in Fig. 14b. The measured phase current/voltage will be considered as the α component and a 90 degree phase shifted signal of the measured quantity to be the β component of the $\alpha\beta$ reference frame. Synthesizing β signal is achieved by storing the samples of α signal in a first-in-first-out (FIFO) buffer; wherein the buffer length is the nearest integer to $\frac{1}{4 f_o T_s}$ where T_s is the sampling time.

For single phase systems that uses the above mentioned split phase technique to represent in the SRF, the Fully DP and DP-DQ method can suffer from reduced accuracy since the space phasors are not well defined in the transient due to the delayed β component. The DP-EMT method does not

suffer from this disadvantage since the control implementation is same as the real-world implementation. For stationary domain controllers, all three closed-loop methods can be used to effectively model the dynamics.
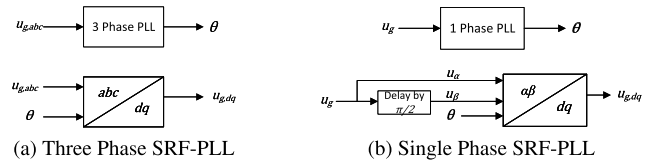
(a) Three Phase SRF-PLL   (b) Single Phase SRF-PLL

FIGURE 14. PLL with the corresponding stationary-dq transformation.

C. APPLICATION TO THREE PHASE POWER CONVERTERS

The SRF-PLL corresponding to the three phase system is shown in Fig. 14b. Since the space phasor is well defined in three phase systems, there are no require of data buffers in the DQ conversion and therefore no interactions in the DQ domain as seen in the single phase case. For three phase converters, Fully DP method can be applied to the SRF-PI controller and stationary-PR controller. Since the stationary-PR controller can be assumed to be equivalent of the SRF-PI [25], the implementation is identical. SRF-SMC and other non-linear controllers are too complex and inefficient to implement through Fully DP method.

For three phase converters, both DP-DQ and DP-EMT can be used to implement all the different controller types effectively and accurately. DP-DQ and DP-EMT are equivalent unless there are filtering in the stationary domain prior to the DQ conversion or delays in obtaining the stationary frame signals. In such a case, DP-EMT could accurately model the closed-loop dynamics.

VI. SIMULATION RESULTS AND VALIDATION

The closed-loop power converter models are validated via time domain simulations. The results obtained are validated against detailed switched EMT models built in MATLAB Simulink. The goal is to validate the transient behavior obtained from the DP models. We particularly focus on the the error between the DP simulation data and EMT simulation data from Simulink during the transient. A step change in the current reference is applied at $t = 0.15s$ and the current samples between the interval $t = 0.15s$ to $t = 0.20s$ are obtained. The NRMSE is calculated according to (27), where N represents the total number of samples and I_{DP}, $I_{Simulink}$ represents the simulation data obtained from proposed DP and Simulink respectively.

$$NRMSE = \frac{\sqrt{\frac{1}{N} \sum_{i=1}^{i=N} \left(I_{DP} - I_{Simulink} \right)^2}}{I_{Simulink,max} - I_{Simulink,min}} \quad (27)$$

The different closed-loop hybrid approaches are validated for different controller types following which their applicability and accuracy are discussed. The DPs of the inverter switched voltage can be calculated for the chosen topology

during the initialisation phase of the simulation. The following steps can be followed during the initialisation:

- Specify the number of grid frequency harmonics and switching harmonics
- Determine the number of bessel function terms required to model the harmonics accurately
- Calculate the phasor magnitudes for all selected frequencies under a nominal control set-point and consider only those frequencies whose phasor magnitudes are greater than the assumed threshold, in this paper, phasor magnitude threshold is 5 percent
- Compute the phasor magnitude and phase for all considered frequencies in the previous step by varying the control variables M_r and φ and store the data in the form of a lookup table

Such a lookup table prevents the calculation of inverter output phasors at each control update. The simulation is executed with a time step of $1\mu s$ and the control update is performed every $100\mu s$.

A. SINGLE PHASE CONVERTER

The parameters of the single phase 2-level converter are shown in Table 2. The control parameter of the single phase inverter are summarized in Table 3. In this case study, the converter is operating in grid-following mode, with a current controller. The output LCL filter of the converter which contains 3 energy storage elements requires 6 DP state variables per frequency. In this study case, we have assumed $m = 6$ and $n = 5$ for the harmonics. Considering the threshold for inverter output harmonics as 5 percent of the nominal for inclusion in the state equation, the number of harmonics are 8 and the number of state equations are 48.

TABLE 2. Parameters of single phase converter.

Parameter	Values	Parameter	Values
v_{dc}	360 V	L_c	0.6 mH
V_{grid}	220 V	L_g	0.15 mH
f_{sw}	10 kHz	C_f	10 μF
f_o	50 Hz	R_c, R_g	0.2 Ω

TABLE 3. Control parameters of single and three phase converter.

Controller	Parameters
PI	$K_p = 0.05$, $K_i = 55.7$
SMC	$K_{smc} = 3.5$
PR	$K_{p,pr} = 0.07$, $K_{i,pr} = 126.9$

The Fully DP strategy is identical to Hybrid DP-DQ for single phase converters in terms of the output response. Fig. 15 shows the post processed capacitor voltage using Hybrid DP-DQ and Fully DP method. It can be seen that the ripples on the capacitor voltage are accurately matching the detailed time domain simulation in Simulink. A step change in the DQ reference current is made at 0.15s and the post-processed current i_c is shown in Fig. 16. From the
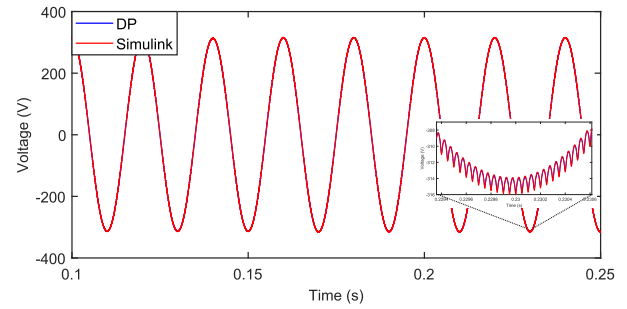

FIGURE 15. Capacitor voltage of single phase converter with SRF PI controller using DP-DQ approach.
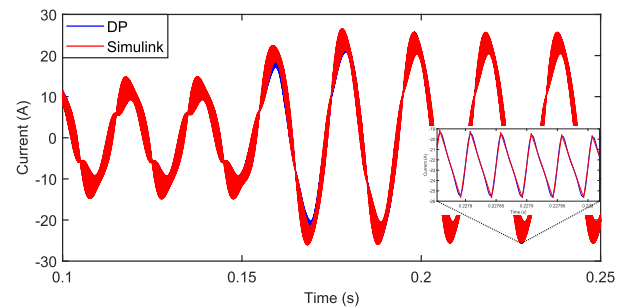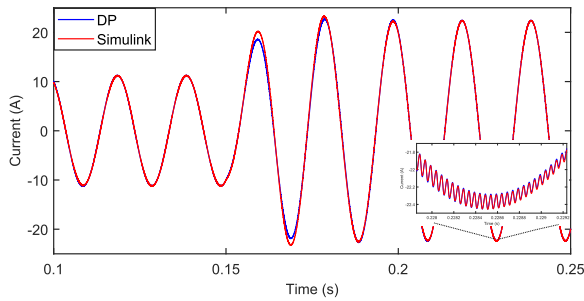

FIGURE 16. Converter current of single phase converter with SRF PI controller using DP-DQ approach.

TABLE 4. Comparison of % NRMSE of hybrid closed-loop methods for various controllers pertaining to single phase converter application.

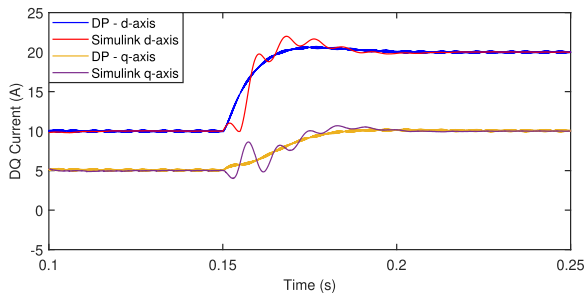| Controller	Fully DP	Hybrid DP-DQ	Hybrid DP-EMT
SRF-PI	1.62 %	1.63 %	0.79 %
SRF-SMC	–	5.62 %	1.1 %
Stationary PR	1.77 %	2.72 %	1.27 %

zoomed portion in Fig. 16, the harmonic on the waveform match the response from Simulink. To accurately the compare the transient behavior between Hybrid DP-DQ and Hybrid DP-EMT method, the comparison of post processed grid current and DQ currents are presented. Fig. 17a and Fig. 17b shows the comparison in grid current. Although the harmonics are matched in both methods, the transient behavior is well matched to Simulink in DP-EMT method. This is further confirmed from the post processed DQ currents as shown in Fig. 17c and Fig. 17d. Furthermore, a comparison of NRMSE for each controller scenario against hybrid modelling approaches are presented in Table 4. When considering the SRF-PI controller, the %NRMSE of hybrid DP-EMT approach is 0.79 % whereas for DP-DQ and Fully DP methods, the %NRMSE is 1.63 %. DP-DQ method does not capture the transient accurately since the controller in SRF domain has a delay buffer prior to DQ conversion. Space phasors are not well defined for single phase systems during the transient. For non-linear control law such as the SRF SMC controller, Fully DP method is not applicable and furthermore the above mentioned effect of external delay is
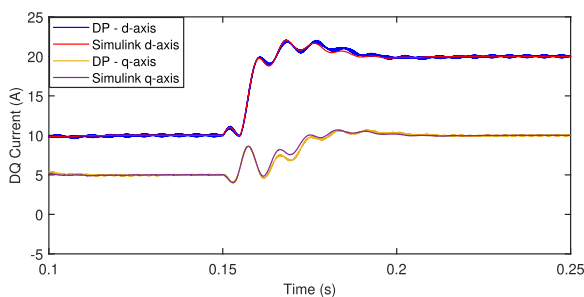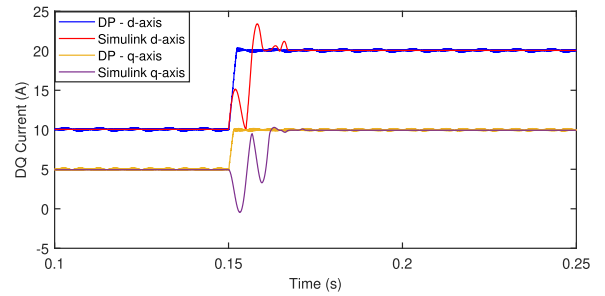
(a) Grid current DP-DQ
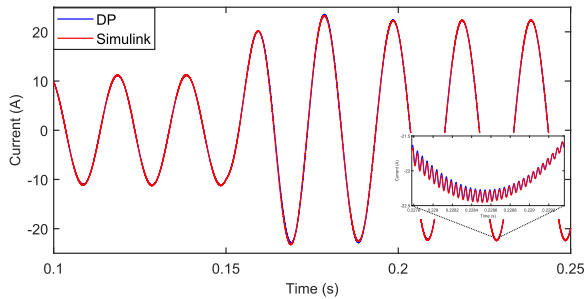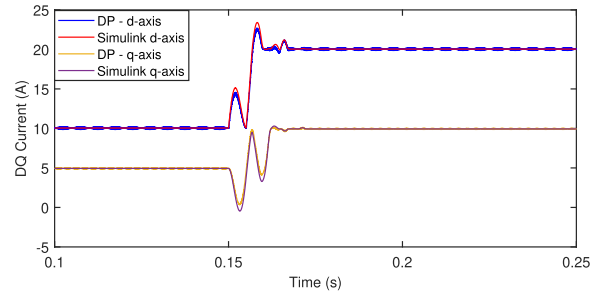

(b) Grid current DP-EMT

(c) DQ current DP-DQ

(d) DQ current DP-EMT

FIGURE 17. Comparison of DP-DQ and DP-EMT approach for single phase converter with SRF PI controller.

(a) DQ current DP-DQ

(b) DQ current DP-EMT

FIGURE 18. Comparison of DP-DQ and DP-EMT approach for single phase converter with SRF SMC controller.

current in the case of DP-DQ is 5.62 % indicating poor accuracy during transients whereas for DP-EMT method, the %NRMSE in grid current is 1.1 % which confirms the accurate transient representation achieved in DP-EMT method when compared to DP-DQ method.

TABLE 5. Parameters of three phase converter.

| Parameter	Values	Parameter	Values
v_{dc}	850 V	L_c	1 mH
V_{grid}	400 V	L_g	0.3 mH
f_{sw}	10 kHz	C_f	20 μF
f_oy	50 Hz	R_c, R_g	0.2 Ω

B. THREE PHASE CONVERTER

Table 5 shows the parameters of the three phase inverter and the control parameters are given in Table 3. We have assumed $m = 6$ and $n = 5$ for the harmonics. Considering the threshold for inverter output harmonics as 5 percent of the fundamental phasor for inclusion in the state equation, the number of harmonics are 7 and the number of state equations are 42 per phase. We have evaluated the three phase converter model similar to the single phase phase converter by testing he controllers with the various hybrid closed-loop methods.

As discussed previously, the Fully DP strategy is not suited for non-linear control law. For three phase systems, the space phasor concept is well defined unlike a single phase system where a 90 degree delayed fictitious signal is required. Due to the well defined space phasors, the hybrid DP-DQ method is found to be highly accurate and equivalent to the Hybrid DP-EMT method. Fig. 19a and Fig. 19b shows the grid

further exaggerated in the output DQ currents with Hybrid DP-DQ method. Fig. 18a shows the DQ current with DP-DQ method for an SRF SMC control. In Fig. 18a, the steady state values obtained from SIMULINK and Hybrid DP-DQ method match however the transient behavior has a significant mismatch. However, with DP-EMT method as shown in Fig. 18b, the DQ current transients are accurately matching the response obtained from SIMULINK. As shown in Table 4, when considering the SMC controller, the %NRMSE of grid

TABLE 6. Comparison of applicability and accuracy of hybrid closed-loop methods for various controllers pertaining to single phase and three phase converter application.

| Controller	Fully DP		Hybrid DP-DQ		Hybrid DP-EMT	
	Single Phase	Three Phase	Single Phase	Three Phase	Single Phase	Three Phase
SRF-PI	Reduced accuracy in transient	Accurate	Reduced accuracy in transient	Accurate	Accurate	Accurate
SRF-SMC	Highly complex	Highly complex	Low accuracy in transient	Accurate	Accurate	Accurate
Stationary PR	Accurate	Accurate	Identical to SRF-PI, reduced accuracy	Identical to SRF-PI, accurate	Accurate	Accurate

current and DQ current with hybrid DP-DQ method during a step change in the DQ current reference. As observed from Fig. 19a and Fig. 19b, the transients are matching accurately. Furthermore, when implemented with the DP-EMT method, no significant improvement is noticed due to the well defined space phasors in a three phase system. Unless the controller is implemented in a stationary frame or unless any signal processing is done in the stationary frame, the DP-DQ method is well suited for three phase systems.
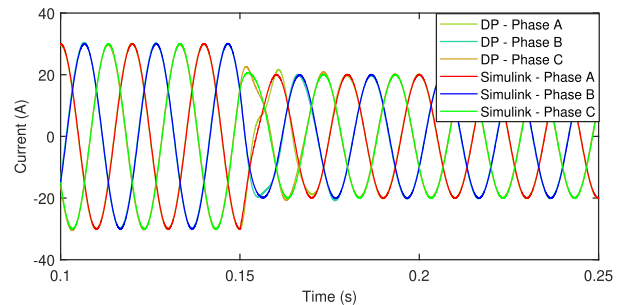

(a) Grid current

(b) DQ current
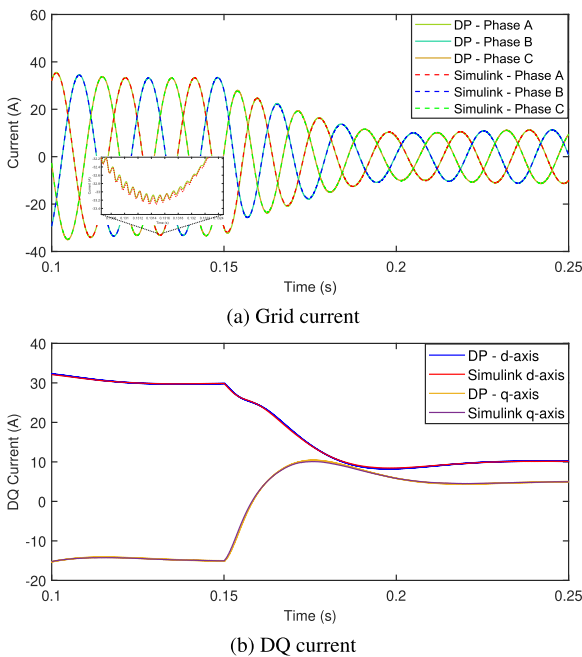
FIGURE 19. DP-DQ approach for three phase converter with SRF PI controller.

The stationary frame PR controller is tested with the DP-EMT method for the three phase converter. Fig. 20 shows the converter output current. As shown in the zoomed waveform in Fig. 20, the ripple in the converter current is exactly matching the simulations in Simulink. Furthermore, the transients also accurately match. The grid current shown in Fig. 21 also matches the steady state and transients simulated from Simulink.

For further validating the accuracy of the proposed hybrid methods, the scenario pertaining to voltage sag for the three
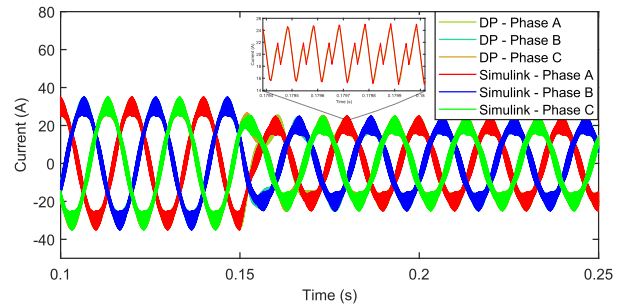
FIGURE 20. Converter current of three phase converter with stationary PR controller using DP-EMT approach.
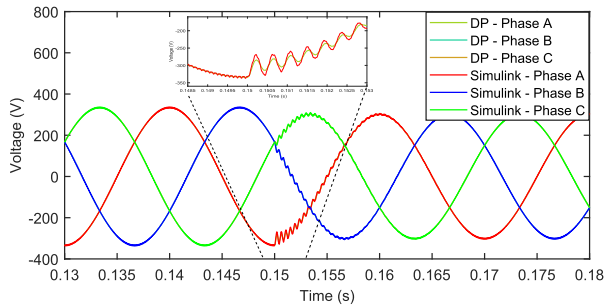

FIGURE 21. Grid current of three phase converter with stationary PR controller using DP-EMT approach.

phase converter is presented. The voltage sag scenario is tested for both the Hybrid DP-DQ and Hybrid DP-EMT methods and tested for different controlled types considered in this paper. As an example, the results obtained for the DP-EMT method considering a PI control is presented. At time $t = 0.15s$, a sudden grid voltage sag of 10 % is considered. As shown in Fig. 22, the capacitor voltage under goes a sudden sag of 10 % at time $t = 0.15s$. As observed in Fig. 22, the transients obtained in Hybrid DP-EMT method matches the transients obtained from Simulink. Due to the PI control action of the current controlled inverter, a constant current of peak 30A is maintained following a transient that arose due to sudden voltage sag as shown in Fig. 23. Fig. 23 shows that the grid current during the voltage sag event obtained from the Hybrid DP-EMT method matches that of Simulink during the transient.

C. DISCUSSION AND RECOMMENDATION

Table 6 summarises the applicability and accuracy of applying hybrid closed loop modelling methods for single phase

FIGURE 22. Capacitor voltage of three phase converter under voltage sag condition with SRF-PI controller using DP-EMT approach.
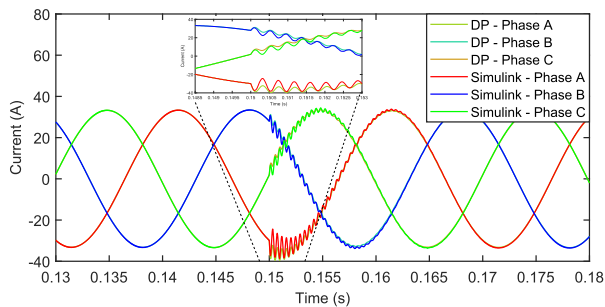
FIGURE 23. Grid current of three phase converter under voltage sag condition with SRF-PI controller using DP-EMT approach.

and three phase systems considering various controller types. As mentioned earlier, the Fully DP method is not suited for non-linear controllers due to the increased complexity arising from the convolution principle. The Fully DP method can be applied effectively to linear controllers in SRF and stationary domain. In single phase systems with controller in SRF domain, the Fully DP method has low accuracy in transient. As shown in Table 6, the hybrid DP-DQ method can be applied to both linear and non-linear controllers. This method is highly accurate for three phase systems unless any signal processing is present in the stationary domain before conversion to DQ domain. However, the DP-DQ method for single phase applications has a drawback of reduced accuracy in transient. Accurate simulations are obtained with the hybrid DP-EMT method method for all controller types and for both single and three phase applications.

Thus, to summarize, we recommend the strategies marked as accurate in Table 6 for single and three phase applications. The hybrid approach that is generic and accurately models the dynamics for all controller types would be the hybrid DP-EMT approach.

To reduce the complexity of the DP-based simulation, two recommendations are proposed for the initialisation phase of the simulation:

- Pre-calculate the required number of fundamental and switching harmonics and estimate the number of bessel terms to accurately model the harmonics. Following the previous step, the significant harmonics that needs to be included can be calculated

- Create a lookup table for the phasor of the switched power converter output voltage with the control inputs. This step can eliminate the calculation of phasors, which involves calculation of Bessel function for every time step which is critical in closed-loop simulations

VII. CONCLUSION AND FUTURE WORK

This paper presents dynamic phasor modelling of single and three phase two level converters and proposes various hybrid closed-loop modelling approaches within the dynamic phasor framework. The applicability and accuracy of the hybrid closed-loop approaches are analysed for different controller types considering single and three phase power converters. Overall, the Hybrid DP-EMT approach is found to be superior compared other strategies. The Hybrid DP-DQ strategy can be used for three phase systems when signal processing is not present in the stationary domain. The proposed hybrid approaches were validated against detailed switched power converter models and NRMSE calculations during the transient were analyzed to characterize the accuracy of each hybrid approach.

This work is currently extended to include higher order DP models of AC electrical motor and auto-transformer rectifier unit (ATRU) which is currently used in the electrical drives of MEAs.

REFERENCES

[1] B. Sarlioglu and C. T. Morris, "More electric aircraft: Review, challenges, and opportunities for commercial transport aircraft," *IEEE Trans. Transport. Electrific.*, vol. 1, no. 1, pp. 54–64, Jun. 2015.

[2] Q. Xu, P. Wang, J. Chen, C. Wen, and M. Y. Lee, "A module-based approach for stability analysis of complex more-electric aircraft power system," *IEEE Trans. Transport. Electrific.*, vol. 3, no. 4, pp. 901–919, Dec. 2017.

[3] J. Sun, M. Chen, and K. J. Karimi, "Aircraft power system harmonics involving single-phase PFC converters," *IEEE Trans. Aerosp. Electron. Syst.*, vol. 44, no. 1, pp. 217–226, Jan. 2008.

[4] S. R. Sanders, J. M. Noworolski, X. Z. Liu, and G. C. Verghese, "Generalized averaging method for power conversion circuits," *IEEE Trans. Power Electron.*, vol. 6, no. 2, pp. 251–259, Apr. 1991.

[5] H. Qin and J. Kimball, "Generalized average modeling of dual active bridge DC–DC converter," *IEEE Trans. Power Electron.*, vol. 27, no. 4, pp. 2078–2084, Aug. 2012.

[6] J. Huang, Y. Wang, Z. Li, and W. Lei, "Multifrequency approximation and average modelling of an isolated bidirectional DC–DC converter for DC microgrids," *IET Power Electron.*, vol. 9, no. 6, pp. 1120–1131, May 2016.

[7] M. Cupelli, S. K. Gurumurthy, and A. Monti, "Modelling and control of single phase DAB based MVDC shipboard power system," in *Proc. 43rd Annu. Conf. IEEE Ind. Electron. Soc.*, Oct. 2017, pp. 6813–6819.

[8] D. G. Holmes and T. A. Lipo, *Pulse Width Modulation for Power Converters: Principles and Practice*, vol. 18. Hoboken, NJ, USA: Wiley, 2003.

[9] X. Ruan, X. Wang, D. Pan, D. Yang, W. Li, and C. Bao, *Control Techniques for LCL-Type Grid-Connected Inverters*. Cham, Switzerland: Springer, 2018.

[10] Q. Luo, Q. Zhong, G. Wang, and L. Wang, "An order-reduction method of interharmonic analysis model based on the principle of interharmonic interaction," *CPSS Trans. Power Electron. Appl.*, vol. 6, no. 3, pp. 209–217, Sep. 2021.

[11] M. Daryabak, S. Filizadeh, J. Jatskevich, A. Davoudi, M. Saeedifard, V. Sood, J. Martinez, D. Aliprantis, J. Cano, and A. Mehrizi-Sani, "Modeling of LCC-HVDC systems using dynamic phasors," *IEEE Trans. Power Del.*, vol. 29, no. 4, pp. 1989–1998, Aug. 2014.

[12] D. Yuan, S. Wang, and Y. Liu, "Dynamic phasor modeling of various multipulse rectifiers and a VSI fed by 18-pulse asymmetrical autotransformer rectifier unit for fast transient analysis," *IEEE Access*, vol. 8, pp. 43145–43155, 2020.

[13] T. Demiray, "Simulation of power system dynamics using dynamic phasor models," Ph.D. dissertation, ETH Zürich, Zürich, Switzerland, 2008.

[14] X. Mao, Y. Wen, L. Wu, and B. Zhou, "Simulation of LCC-MMC HVDC systems using dynamic phasors," *IEEE Access*, vol. 9, pp. 122819–122828, 2021.

[15] Z. Shuai, Y. Peng, J. M. Guerrero, Y. Li, and Z. J. Shen, "Transient response analysis of inverter-based microgrids under unbalanced conditions using a dynamic phasor model," *IEEE Trans. Ind. Electron.*, vol. 66, no. 4, pp. 2868–2879, Apr. 2019.

[16] M. A. Kulasza, U. D. Annakkage, and C. Karawita, "Extending the frequency bandwidth of transient stability simulation using dynamic phasors," *IEEE Trans. Power Syst.*, vol. 37, no. 1, pp. 249–259, Jan. 2021.

[17] A. Monti, F. Milano, E. Bompard, and X. Guillaud, *Converter-Based Dynamics and Control of Modern Power Systems*. New York, NY, USA: Academic, 2020.

[18] X. Wang and F. Blaabjerg, "Harmonic stability in power electronic-based power systems: Concept, modeling, and analysis," *IEEE Trans. Smart Grid*, vol. 10, no. 3, pp. 2858–2870, May 2018.

[19] C. Shah, J. D. Vasquez-Plaza, D. D. Campo-Ossa, J. F. Patarroyo-Montenegro, N. Guruwacharya, N. Bhujel, R. D. Trevizan, F. A. Rengifo, M. Shirazi, R. Tonkoski, R. Wies, T. M. Hansen, and P. Cicilio, "Review of dynamic and transient modeling of power electronic converters for converter dominated power systems," *IEEE Access*, vol. 9, pp. 82094–82117, 2021.

[20] D. Shu, X. Xie, V. Dinavahi, C. Zhang, X. Ye, and Q. Jiang, "Dynamic phasor based interface model for EMT and transient stability hybrid simulations," *IEEE Trans. Power Syst.*, vol. 33, no. 4, pp. 3930–3939, Jul. 2018.

[21] Q. Huang and V. Vittal, "Advanced EMT and phasor-domain hybrid simulation with simulation mode switching capability for transmission and distribution systems," *IEEE Trans. Power Syst.*, vol. 33, no. 6, pp. 6298–6308, Nov. 2018.

[22] T. J. Member, S. Xinya, J. Willkomm, S. Schlegel, and D. Westermann, "Hybrids-simulation using EMT—And phasor-based model for converter dominated distribution grid," in *Proc. IEEE PES Innov. Smart Grid Technol. Conf. Eur. (ISGT-Eur.)*, Oct. 2018, pp. 1–6.

[23] J. R. Martí, H. W. Dommel, B. D. Bonatto, and A. F. R. Barrete, "Shifted frequency analysis (SFA) concepts for EMTP modelling and simulation of power system dynamics," in *Proc. Power Syst. Comput. Conf.*, Aug. 2014, pp. 1–8.

[24] A. Nazari, Y. Xue, J. K. Motwani, I. Cvetkovic, D. Dong, and D. Boroyevich, "Dynamic phasor modeling of three phase voltage source inverters," in *Proc. 6th IEEE Workshop Electron. Grid (eGRID)*, Nov. 2021, pp. 1–6.

[25] D. G. Holmes, T. A. Lipo, B. P. McGrath, and W. Y. Kong, "Optimized design of stationary frame three phase AC current regulators," *IEEE Trans. Power Electron.*, vol. 24, no. 11, pp. 2417–2426, Nov. 2009.

[26] C. Zou, B. Liu, S. Duan, and R. Li, "Stationary frame equivalent model of proportional-integral controller in dq synchronous frame," *IEEE Trans. Power Electron.*, vol. 29, no. 9, pp. 4461–4465, Sep. 2014.

MARKUS MIRZ received the Ph.D. degree in engineering from RWTH Aachen University, in 2020.

He is currently leading the Research Groups with the Fraunhofer Center for Digital Energy and the Institute for Automation of Complex Power Systems, RWTH Aachen University. His research interests include the area of power system real-time simulation, modeling, and automation software solutions.

BERNARD S. AMEVOR received the B.S. degree in electrical and electronics engineering from the Kwame Nkrumah University of Science and Technology, Ghana, in 2017. He is currently pursuing the M.Sc. degree in electrical engineering with RWTH Aachen University.

His research interests include modeling, control, and simulation of power electronics and electrical drives.

FERDINANDA PONCI (Senior Member, IEEE) received the Ph.D. degree in electrical engineering from the Politecnico di Milano, Italy, in 2002.

She joined the Department of Electrical Engineering, University of South Carolina, Columbia, SC, USA, as an Assistant Professor, in 2003, and was a tenured promoted in 2008. In 2009, she joined the E.ON Research Center, Institute for Automation of Complex Power Systems, RWTH Aachen University, Aachen, Germany, where she is currently a Professor for monitoring and distributed control for power systems. Her research interests include advanced measurement, monitoring, and automation of active distribution systems.

Dr. Ponci is an Elected Member of the Administration Committee of the IEEE Instrumentation and Measurement Society and the Liaison with IEEE Women in Engineering.

ANTONELLO MONTI (Senior Member, IEEE) received the M.Sc. degree *(summa cum laude)* and the Ph.D. degree in electrical engineering from the Politecnico di Milano, Italy, in 1989 and 1994, respectively.

He started his career in Ansaldo Industria and then moved to the Politecnico di Milano, as an Assistant Professor, in 1995. In 2000, he joined the Department of Electrical Engineering of the University of South Carolina (USA) as an Associate and then a Full Professor. Since 2008, he has been the Director of the E.ON Energy Research Center, Institute for Automation of Complex Power System, RWTH Aachen University. Since 2019, he holds a double appointment with Fraunhofer FIT, where he is developing the new Center for Digital Energy, Aachen. He is the author or coauthor of more than 400 peer-reviewed papers published in international journals and in the proceedings of international conferences. He is an Associate Editor of *IEEE Electrification Magazine*, a member of the Editorial Board of the *SEGAN* journal (Elsevier), and a member of the Founding Board of the *Energy Informatics* journal (Springer). He was a recipient of the 2017 IEEE Innovation in Societal Infrastructure Award.

SRIRAM KARTHIK GURUMURTHY (Member, IEEE) received the M.Sc. degree in electrical power engineering from RWTH Aachen University, Aachen, Germany, in 2017.

He is currently a Research Associate with the E.ON Energy Research Center, Institute for Automation of Complex Power Systems, RWTH Aachen University. His research interests include modeling, control, stability analysis, and automation of power electronics-driven power systems.